Hardness and fracture toughness of solid solutions of Mg_2Si and Mg_2Sn

Gustavo Castillo Hernandez[1,2], Mohammad Yasseri[1,2], Sahar Ayachi[1], Johannes de Boor[1], Eckhard Müller[1,2]

[1] Institute of Materials Research, German Aerospace Center, 51170 Cologne, Germany
[2] Institute of Inorganic and Analytical Chemistry, Justus Liebig University Giessen, Heinrich-Buff-Ring 17, 35392 Giessen, Germany

Abstract

Thermoelectric material development typically aims at maximizing produced electrical power and efficiency of energy conversion, even though sometimes, this means adding expensive or toxic materials. An alternative is to use highly available and low toxic silicides. In fact, magnesium silicide and magnesium stannide have low densities (1.99 and 3.49 g/cm^3 respectively), and exhibit good thermoelectric properties with their thermoelectric figure of merit zT>1 for n-type and near 0.6 for p-type Mg_2Si-Mg_2Sn solid solutions in the range of 723-773 K. These properties turn the materials into logical candidates for light-weight and efficient thermoelectric generators (TEG). The research on their mechanical properties is however lagging behind and little effort has been put into understanding them. In this work we study the effect of the composition over the Mg_2Si-Mg_2Sn solid solution series on hardness and fracture toughness values. Hardness ranges from 2.44-5.56 GPa whereas fracture toughness values are in a tighter range (0.64-0.88 MPam$^{1/2}$). However, the highest value does not belong to binary Mg_2Si but a composition within the solid solution that exhibits secondary phase nanostructuring.

1. Introduction

Thermoelectric materials have been studied for a long time as a means of reusing waste heat and converting it to electricity. From the variety of materials available for such effect, magnesium alloys such as Mg_2Si, Mg_2Sn and Mg_2Ge [1] started to attract attention lately because of their light weight, high abundance, negligible toxicity [2, 3] and their similar crystal structure. They form solid solutions with improved thermoelectric properties compared to the corresponding binary compounds [1, 4]. Most of the materials research is focused on improving thermoelectric properties [5-11], whereas mechanical properties received little attention to date even though they are also crucial for the development of durable thermoelectric generators (TEG).

Thermoelectric materials in TEG operation are subjected to a variety of mechanical and thermal stresses [12, 13] caused by thermal expansion coefficient mismatch, thermal cycling, and static and dynamic mechanical loads. Materials must be able to withstand such stresses for a long service life.

Mechanical loading of the material is expected to create micro-cracking within the material [14], and previous studies show that crack appearances in the material lead to performance decay [15, 16]. Moreover, the failure mode for brittle materials has been described as the appearance and growth of such cracks [17]. Therefore it is of utmost importance to characterize the mechanical properties exhibited by thermoelectrics on-par with their energy conversion optimization.

It is commonly established that elastic properties such as Young's modulus and shear modulus, as well as the surface hardness and fracture toughness, are good indicators of a material´s ability to withstand loads [18].

Magnesium silicide is a well-known material whose mechanical properties have been predicted using First principles calculations (110 GPa for the Young´s modulus) [19] and experimentally studied using

resonant ultrasound spectroscopy [20, 21], hardness testing [22] and compression tests [23]. These methods yielded several Young´s modulus values, ranging from 76 GPa for induction melted cast material up to 145 GPa for SPS, with their corresponding hardness values of 4 GPa and 5,4 GPa. The difference was attributed by the authors to differences in grain size, as spark plasma sintering produces very small grains while cast material promotes grain growth.

On the other hand, research for Mg_2Sn has a more limited literature than Mg_2Si. First principles calculations for this binary show a Young´s modulus of 82 GPa [24] and a hardness of 1,7 GPa [25]. The solid solutions Mg_2Si-Mg_2Sn are attracting attention due to the reported band convergence, the known miscibility gap and the increased performance compared to the binary compounds [1, 5, 7, 26]. However this interest has yet to be more widely extended towards the mechanical properties. Gao *et al.* report the hardness and Young´s modulus in $Mg_2Si_{0.4}Sn_{0.6}$ as 3.07 GPa and 90 GPa, respectively.

This lack of information coupled with the ever better thermoelectric properties obtained for the material system prompts this work to study the mechanical properties exhibited by the binaries Mg_2Si and Mg_2Sn, as well as some compositions along the solid solution series by micro hardness testing using Vickers indentation. By describing the effect of the variation of Si:Sn ratio within the solid solutions we aim at another possibility of nano-structuring that will produce a mechanically stable and robust material for TE generation. Potential candidates from the wide range of compositions were identified through previous research [27, 28].

2. Materials and methods

Undoped $Mg_2Si_xSn_{1-x}$ solid solutions with x = 0, 0.4, 0.5, 0.6, 0.7, 1 were synthesized by mechanical alloying, employing high energy ball milling (SPEX 8000D). The precursors (Mg turnings (Merck), Si (< 6 mm, ChemPUR), Sn (<71 µm, Merck)) were weighed according to stoichiometry. 5% excess of Mg was added as to account for any type of Mg loss during processing and pressing for all compositions, except Mg_2Sn, which had 7.5% excess. The desired elements were transferred into a stainless steel jar with a ball to powder ratio 1.7:1. All the procedures were conducted inside a glove box under Ar atmosphere to prevent oxidation and contamination.

The elements were milled with constant rotation speed (~800 rpm) for 10-12 h until fine and homogeneous powders were obtained. Details for the complete milling are given elsewhere [27]. The obtained powders were transferred to a graphite die (Ø 10 mm) and sintered at 873 - 1073 K by utilizing a direct sinter press DSP 510 SE, Dr. Fritsch GmbH, Fellbach, Germany under vacuum condition (~10^{-5} bar), at a sintering pressure of 66 MPa with a heating rate of 1 K/s. **Table 1** contains the pressing conditions for all samples as well as densities measured by Archimedes method in ethanol.

Table 1. *Pressing parameters and achieved density of compacted $Mg_2Si_{1-x}Sn_X$ pellets*

$Mg_2Si_{1-x}Sn_x$ X	Temperature (K)	Time (s)	Density (g/cm^3)
0	1073	600	1.959
0.4	998	1800	2.597
0.5	973	1200	2.744
0.6	973	1200	2.909
0.7	973	600	3.012
1	873	600	3.425

Pellets were cut using a precision diamond wire cutter (Well Diamond Wire Saws SA) into pieces measuring 2 mm in thickness and then embedded in conductive polymer in pairs. Each pair displayed both the cross section and the surface of the pellet (parallel and perpendicular to the pressing direction). The embedded samples were then ground using SiC paper and polished with ethanol based diamond suspension down to a polish particle size of 0.25 µm.

Hardness testing was done using a Vickers micro hardness machine (Clemex SMT-X7) for 10 s and 0.98 N. Each sample was indented 20 times for each surface orientation (parallel and perpendicular to pressing) for a total of 40 indentations per composition. Imprint analysis was done using the in-built microscope and software, and calculations were done following Oliver and Pharr methodology [29] using Eq 1. to estimate sample hardness

$$H = \frac{1.854 \cdot P}{(2d)^2} \qquad (1)$$

where *P* is the load exerted by the machine and d being the half length of the plastic imprint left by the indentation. Fracture toughness was estimated using Eq 2.

$$K_{Ic} = \frac{\zeta (E/H)^{\frac{1}{2}} P}{c^{3/2}} \qquad (2)$$

where ζ is a geometrical constant estimated to be 0,016 for the Vickers indenter by previous research [29], and *H* is the hardness obtained from Eq 1. *P* is the load, *c* is the half average crack length measured from the center of the imprint and *E* is the Young's modulus estimated in this work by linearly interpolating between theoretical values obtained from previous first principles calculations [19, 24] as shown in **Table 2**. It is assumed that a linear behavior will be dominant since previous research shows this trend for other properties [30].

Table 2. *Young's modulus used to estimate fracture toughness*

$Mg_2Si_{1-x}Sn_x$ *x*	Young's modulus (GPa)
0	110
0.4	98.8
0.5	96
0.6	93.2
0.7	90.4
1	80

Microstructure analysis was carried out using a Scanning Electron Microscope Zeiss Ultra 55 SEM with a Zeiss QBSE detector, also equipped with an Oxford energy dispersive X-ray (EDX) detector (PentaFETx3).

3. Results

As first observation in this study, we found no significant change between measurements done on the cross section and the base face of the pellet as shown in **Figure 1**. This is mainly because of the cubic isotropic nature of the material. Therefore results shall be addressed as a function of composition only.

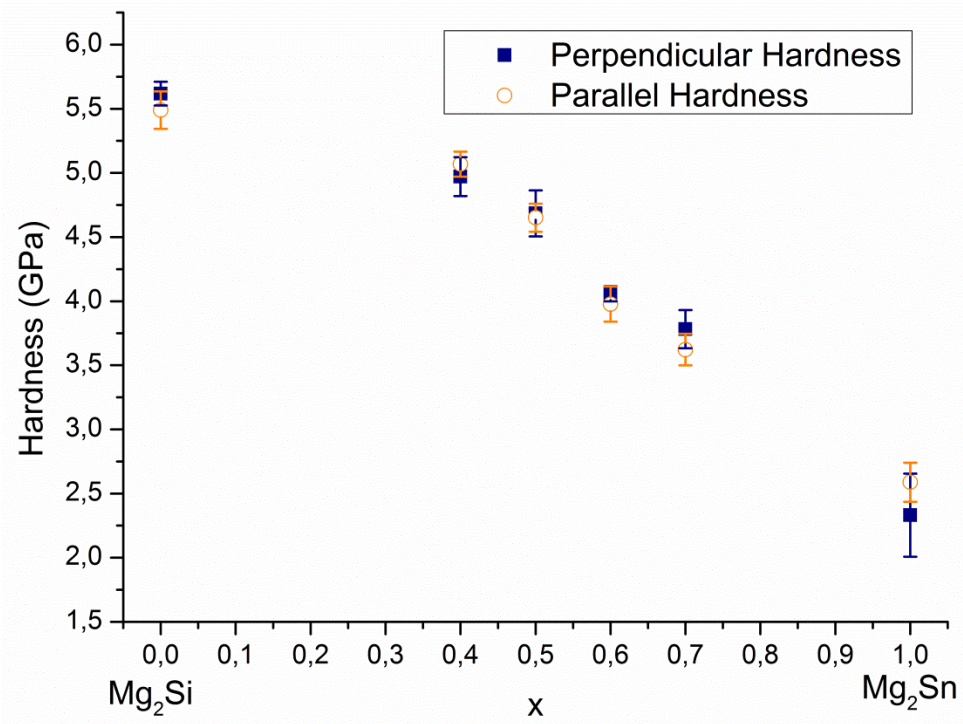

Figure 1. *Comparison between all compositions and the directional (parallel and perpendicular to pressing direction) characterization.*

Using the in-built software, each of the diagonals in every indentation was measured. Afterwards hardness values were calculated using the known force applied. **Figure 2** shows an optical micrograph of an indentation showing the typical radial crack appearance at the tips of the imprint.

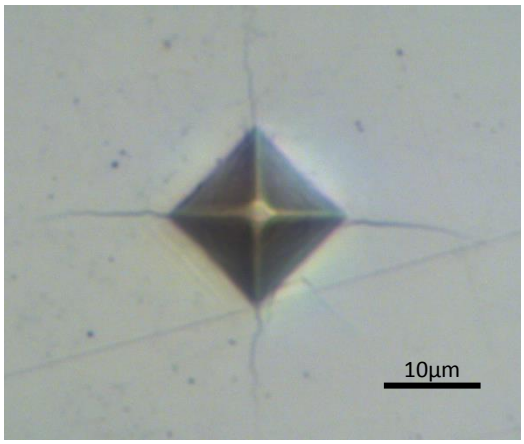

***Figure 2**. Optical micrograph of an Mg_2Si indentation*

Given the brittle nature of the material, scarce strengthening effects are noted in **Figure 2**.
Intrinsic strengthening, acting ahead of the crack tip is seldom found in ceramic materials since it relies on the material´s ability to plastically deform, therefore weak when present. It is however possible to induce crack deviation by using secondary phases or by reducing grain size [31].

As expected from the known behavior in other properties like lattice parameter [30], hardness has a mainly linear behavior with the increase of the Sn content over the solid solution as shown in **Figure 3,**; except for the points *x*=0.5 and 0.4. As the material forms by diffusion of Si into the Mg_2Sn matrix;

the secondary phases are smaller in size and number in low Si content samples. However, increasing the Si:Sn ratio also increases this Si-rich areas in both size and number, also increasing both the hardness and fracture toughness.

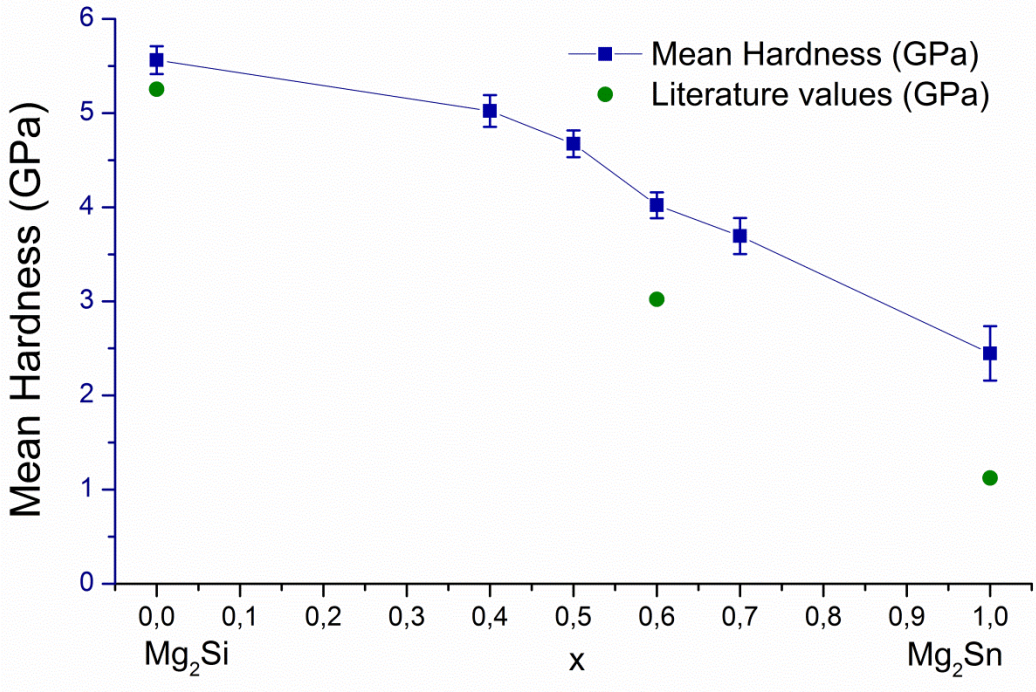

***Figure 3**. Measured hardness values (black squares) compared to literature values (red circles) for Mg_2Si [20], Mg_2Sn [24] and $Mg_2Si_{0.4}Sn_{0.6}$ [25]*

Figure 4 shows the fracture toughness of some compositions along the solid solution series. Here the difference between the binaries is smaller compared to hardness and is related to the tradeoff between the amounts of plastic deformation as compared to the crack length.

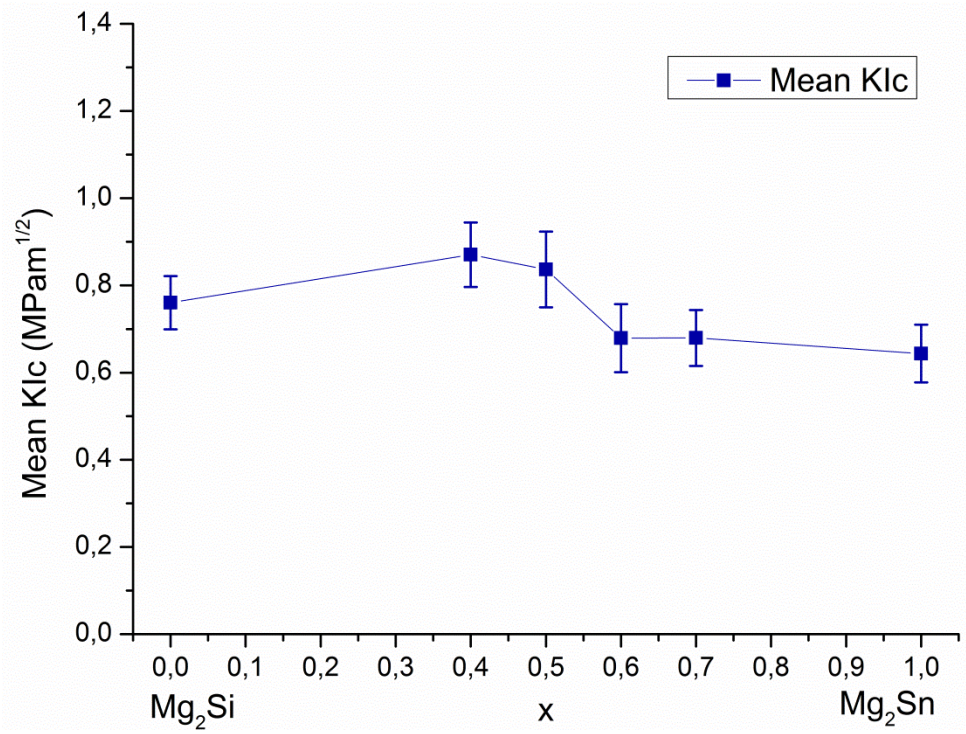

***Figure 4**. Fracture toughness over the solid solution series as a function of composition*

These values have a peculiar behavior around x = 0.5-0.4 which can be attributed to the strengthening effect exerted by the Si rich areas in the material as shown in **Figure 5**.

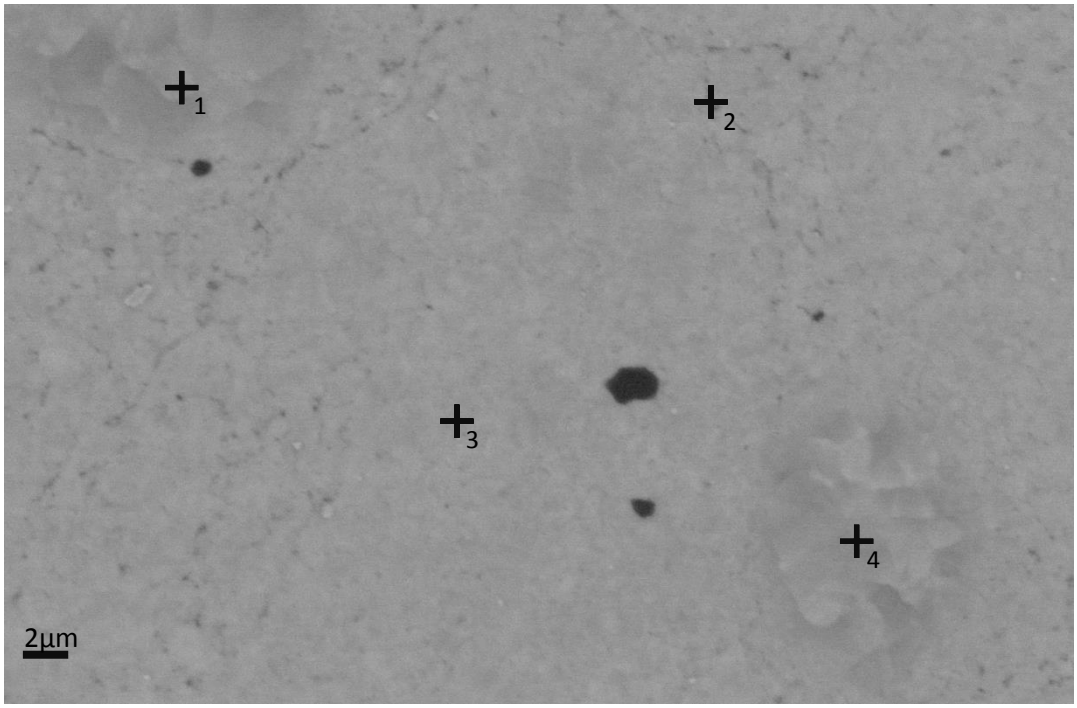

***Figure 5**. SEM picture and EDX points of a nominally $Mg_2Si_{0.6}Sn_{0.4}$ sample with secondary phases present*

The area around EDX point 3 has the composition $Mg_2Si_{0.6}Sn_{0.4}$; while two areas with clear contrast difference can be seen near points 1 and 4. These regions have composition that ranges between $Mg_2Si_{0.75}Sn_{0.25}$ (dark gray area) and $Mg_2Si_{0.51}Sn_{0.48}$ (light gray). The dark areas visible near point 2 are $Mg_2Si_{1-x}Sn_x$ + MgO, and the dark spots in the center of the picture are MgO particles.

4. Discussion

Deviation from linearity in hardness with composition (**Figure 3**) can be expected in non-uniform material with secondary phases. SEM images show regions within the homogenous material that retain a higher content of silicon that was not diffused into the matrix during the high energy ball mill and the following current assisted sintering. Previous reports also show an influence of both milling time and sintering parameters on the thermoelectric properties [27, 30]. Prevalence of these Si rich areas was observed with lower milling time in the same material system where they did not cause any significant change in either the thermal conductivity or electrical properties. Their influence on the mechanical properties is however higher due to the stress fields they produce around the area where they are located.

DSP sintered materials show a slightly larger grain size compared to SPS reports [32] and the mechanical properties decrease accordingly. However, they are better compared to cast material with a typical large grain size [23]. Therefore material synthesis and pressing plays a critical role in the properties exhibited by thermoelectric materials.

Literature values for the hardness of the binary Mg_2Si vary with a low estimate being 3.96 GPa [23], while most values are around 5 GPa [20-22, 32]. In our case, the value of 5.56 ± 0.14 GPa is within a reasonable range. Previous studies have shown that hardness is influenced by grain size; and that smaller grain size results in a higher hardness value. This is related to the amount of plastic deformation allowed by the system. In fact, smaller grains have lower possibility to deform further and are restrained from moving, therefore hardening the material.

Mg_2Sn literature values for hardness are scarce and one study [33] gives a value of 1.17 GPa. Our measured value, however, was comparatively higher with 2.44 ± 0.28 GPa, which is a 100% increase from the literature value. This after mentioned study was done on a magnesium alloy with tin inclusions and not an intentionally synthetized binary stannide for thermoelectric applications, which might be the cause of the deviation.

Fracture toughness values were obtained using the interpolated value for Young´s modulus from first principles calculations. It is possible that a variation in the concentration of secondary phases within the material influenced the elastic properties. Therefore this is another source of variation for the results presented in this work.

Values for K_{Ic} in the binary Mg_2Si range between 0.8 and 1.7 $MPam^{1/2}$ for pristine material [20-22, 32] where our material falls within the lower part of the interval at 0.76 ± 0.06 $MPam^{1/2}$. Current-assisted sintering produces larger grains (1-10 µm) compared to an SPS previous report [32] and it is known that a smaller grain size prevents crack growth [22, 31] which might be behind this lower value.

In pristine binary Mg_2Sn, there are, to the best of our knowledge, no values reported for fracture toughness. Our samples exhibited a value of 0.64 ± 0.06 $MPam^{1/2}$. This value is very similar to Mg_2Si, which might be caused by the lower brittleness exhibited by the material. The work being applied to the material by the indentation can either be released as plastic deformation (imprint) or as new surfaces (cracks). The value for Young´s modulus is reduced in a similar ratio to the hardness, thus, according to Eq. 2, the fracture toughness will remain comparatively high.

Crack lengths for both silicide (22.7 ± 2.1 µm) and stannide (26.99 ± 3.54 µm) remained similar. The imprint size, however, was not. Magnesium silicide has a noticeably smaller residual deformation (1.80 ± 0.02 µm) compared to the magnesium stannide (27.41 ± 0.46 µm).

Brittle materials like magnesium silicide-stannide have a very low plastic deformation capability and therefore, the only way to strengthen them intrinsically is to include flaws in the lattice. A change in direction due to a pinned stress field caused by the grain boundary is the main strengthening factor in a single phase material with no inclusions [31] (**Figure 5 c**). The coexistence of several phases in the material strengthens it against crack growth by this very same method, as the crack is forced to go through several stress fields (phase boundaries) caused by the phase mismatch (**Figure 5 b**).

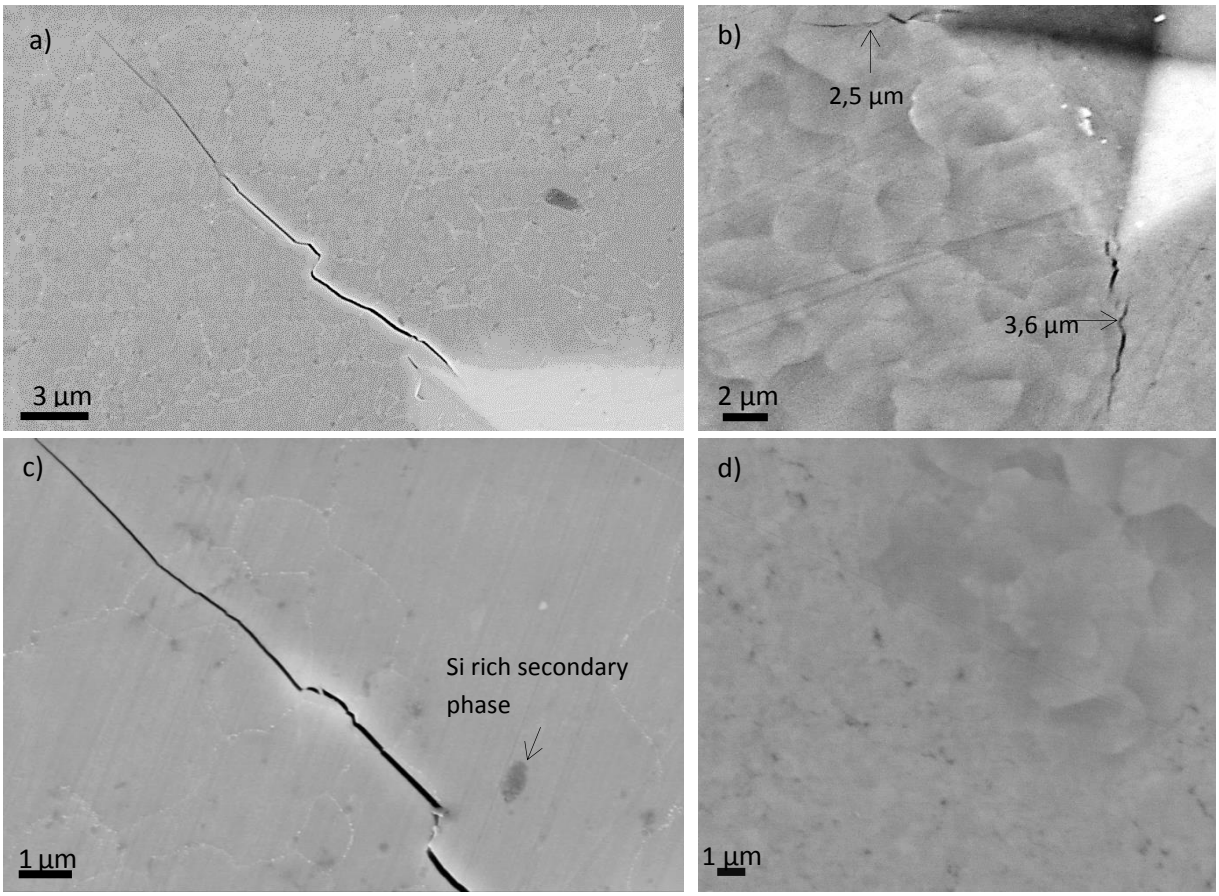

***Figure 5**. SEM pictures showing the comparison between a homogenous $Mg_2Si_{0.3}Sn_{0.7}$ material (a and c) compared to an $Mg_2Si_{0.6}Sn_{0.4}$ material with secondary phases (b and d). Note the difference in crack length*

Magnesium silicide-stannide ranks somewhere in the middle within other thermoelectric material families regarding hardness values. They are clearly above tellurides which exhibit a value ranging from 0.7-1.5 GPa [34, 35], have a comparable hardness value to Skutterudites (3-7 GPa) [35, 36], and are below half-Heuslers which can surpass 10 GPa [35, 37].

When comparing fracture toughness exhibited by different thermoelectric materials, we find the Mg_2Si-Mg_2Sn system to be at the lower end, having a lower value than half-Heuslers (1.8-2 $MPam^{1/2}$) [37] and tellurides (1.1 $MPam^{1/2}$) [38]. However, they are comparable to Skutterudites (0.4-0.8 $MPam^{1/2}$) [39].

5. Conclusion

Different compositions of magnesium silicide–magnesium stannide solid solutions were successfully synthetized and characterized. They exhibited medium to low hardness and low fracture toughness when compared to other thermoelectric materials. In this work, the first ever report of the fracture toughness in magnesium stannide binary compound was discussed.

Magnesium silicide is a very brittle material with a high hardness value, whereas magnesium stannide has a lower brittleness. However, both have similar fracture toughness due to the fact that Mg_2Sn is capable of more plastic deformation compared to Mg_2Si.

Considerable strengthening effect of secondary phases was observed in higher silicon content samples. This was credited to interphase stress shortening and deflecting crack growth. Secondary phases that do not interfere with thermoelectric properties can thus exert a beneficial effect of a shortened material preparation.

Further work is needed to strengthen the material through microstructure optimization or nano-inclusions, and complement the low density and low toxicity properties that make it an attractive TE material. Mechanical properties should be tailored to the application desired. This in turn, prompts the scientific community to deepen the knowledge in the subject, to be able to engineer the material to specification both in thermoelectric and mechanical properties.

This study shed light on the material mechanical properties and its place among other potential candidates for TE generator materials in relation to how well they manage crack nucleation and growth.

Acknowledgements

The authors would like to thank Dr. Ulises Alfaro Mercado and Reinhard Sottong for the technical support, as well as Alexander Francke for sample preparation and Dr. Alexander Burkov for the kind invitation to the conference. We would also like the acknowledge the endorsement for the DLR executive Board Members for Space Research and Technology, as well as the financial support from the Young Research Group Leader Program.

Financial support for M.Y is provided by the DFG via the GRK (Research Training Group) 2204 "Substitute Materials for Sustainable Energy Technologies“. GCH would like to thank the Mexican science and technology council (CONACyT) and the German academic exchange service (DAAD) for the PhD fellowship.

6. References

[1] J. Mao, H. S. Kim, J. Shuai, Z. H. Liu, R. He, U. Saparamadu, F. Tian, W. S. Liu, and Z. F. Ren, "Thermoelectric properties of materials near the band crossing line in Mg2Sn-Mg2Ge-Mg2Si system," *Acta Materialia,* vol. 103, pp. 633-642, Jan 15 2016.

[2] S. LeBlanc, S. K. Yee, M. L. Scullin, C. Dames, and K. E. Goodson, "Material and manufacturing cost considerations for thermoelectrics," *Renewable & Sustainable Energy Reviews,* vol. 32, pp. 313-327, Apr 2014.

[3] R. Santos, S. A. Yamini, and S. X. Dou, "Recent progress in magnesium-based thermoelectric materials," *Journal of Materials Chemistry A,* vol. 6, pp. 3328-3341, Feb 28 2018.

[4] H. Kasai, L. R. Song, H. L. Andersen, H. Yin, and B. B. Iversen, "Multi-temperature structure of thermoelectric Mg2Si and Mg2Sn," *Acta Crystallographica Section B-Structural Science Crystal Engineering and Materials,* vol. 73, pp. 1158-1163, Dec 2017.

[5] M. I. Fedorov, V. K. Zaitsev, and G. N. Isachenko, "High effective thermoelectrics based on the Mg2Si-Mg2Sn solid solution," *Solid Compounds of Transition Elements,* vol. 170, pp. 286-292, 2011.

[6] V. K. Zaitsev, M. I. Fedorov, E. A. Gurieva, I. S. Eremin, P. P. Konstantinov, A. Y. Samunin, and M. V. Vedernikov, "Highly effective Mg2Si1-xSnx thermoelectrics," *Physical Review B,* vol. 74, Jul 2006.

[7] V. K. Zaitsev, M. I. Fedorov, E. A. Gurieva, I. S. Eremin, P. P. Konstantinov, A. Y. Samunin, and M. V. Vedernikov, "Thermoelectrics of n-type with ZT > 1 based on Mg2Si-Mg2Sn solid solutions," *ICT: 2005 24th International Conference on Thermoelectrics,* pp. 189-195, 2005.

[8] U. Saparamadu, J. de Boor, J. Mao, S. W. Song, F. Tian, W. S. Liu, Q. Y. Zhang, and Z. F. Ren, "Comparative studies on thermoelectric properties of p-type Mg2Sn0.75Ge0.25 doped with lithium, sodium, and gallium," *Acta Materialia,* vol. 141, pp. 154-162, Dec 2017.

[9] J. de Boor, C. Compere, T. Dasgupta, C. Stiewe, H. Kolb, A. Schmitz, and E. Mueller, "Fabrication parameters for optimized thermoelectric Mg2Si," *Journal of Materials Science,* vol. 49, pp. 3196-3204, Apr 2014.

[10] J. de Boor, S. Gupta, H. Kolb, T. Dasgupt, and E. Muller, "Thermoelectric transport and microstructure of optimized Mg2Si0.8Sn0.2," *Journal of Materials Chemistry C,* vol. 3, pp. 10467-10475, 2015.

[11] B. Klobes, J. de Boor, A. Alatas, M. Y. Hu, R. E. Simon, and R. P. Hermann, "Lattice dynamics and elasticity in thermoelectric Mg2Si1-xSnx," *Physical Review Materials,* vol. 3, Feb 28 2019.

[12] T. Sakamoto, T. Iida, Y. Ohno, M. Ishikawa, Y. Kogo, N. Hirayama, K. Arai, T. Nakamura, K. Nishio, and Y. Takanashi, "Stress Analysis and Output Power Measurement of an n-Mg2Si Thermoelectric Power Generator with an Unconventional Structure," *Journal of Electronic Materials,* vol. 43, pp. 1620-1629, Jun 2014.

[13] G. Skomedal, L. Holmgren, H. Middleton, I. S. Eremin, G. N. Isachenko, M. Jaegle, K. Tarantik, N. Vlachos, M. Manoli, T. Kyratsi, D. Berthebaud, N. Y. D. Truong, and F. Gascoin, "Design, assembly and characterization of silicide-based thermoelectric modules," *Energy Conversion and Management,* vol. 110, pp. 13-21, Feb 15 2016.

[14] T. J. Lu and N. A. Fleck, "The thermal shock resistance of solids," *Acta Materialia,* vol. 46, pp. 4755-4768, Aug 10 1998.

[15] E. D. Case, "Thermal Fatigue and Waste Heat Recovery via Thermoelectrics," *Journal of Electronic Materials,* vol. 41, pp. 1811-1819, Jun 2012.

[16] A. B. Zhang, B. L. Wang, J. Wang, J. K. Du, and C. Xie, "Effect of cracking on the thermoelectric conversion efficiency of thermoelectric materials," *Journal of Applied Physics,* vol. 121, Jan 28 2017.

[17] J. P. Singh, C. Shih, and D. P. H. Hasselman, "Analysis of Effect of Crack Interaction on Nature of Strength Loss in Thermally Shocked Brittle Ceramics," *Journal of the American Ceramic Society,* vol. 64, pp. C106-C109, 1981.

[18] M. Edwards and K. Brinkfeldt, "Thermo-Mechanical Modelling and Design of SiGe-based Thermo-Electric Modules for High Temperature Applications," *2013 14th International Conference on Thermal, Mechanical and Multi-Physics Simulation and Experiments in Microelectronics and Microsystems (Eurosime),* 2013.

[19] Z. W. Huang, Y. H. Zhao, H. Hou, and P. D. Han, "Electronic structural, elastic properties and thermodynamics of Mg17Al12, Mg2Si and Al2Y phases from first-principles calculations," *Physica B-Condensed Matter,* vol. 407, pp. 1075-1081, Apr 1 2012.

[20] R. D. Schmidt, E. D. Case, J. Giles, J. E. Ni, and T. P. Hogan, "Room-Temperature Mechanical Properties and Slow Crack Growth Behavior of Mg2Si Thermoelectric Materials," *Journal of Electronic Materials,* vol. 41, pp. 1210-1216, Jun 2012.

[21] R. D. Schmidt, X. F. Fan, E. D. Case, and P. B. Sarac, "Mechanical properties of Mg2Si thermoelectric materials with the addition of 0-4 vol% silicon carbide nanoparticles (SiCNP)," *Journal of Materials Science,* vol. 50, pp. 4034-4046, Jun 2015.

[22] S. Muthiah, R. C. Singh, B. D. Pathak, and A. Dhar, "Mechanical properties of thermoelectric n-type magnesium silicide synthesized employing in situ spark plasma reaction sintering," *Materials Research Express,* vol. 4, Jul 2017.

[23] V. Milekhine, M. I. Onsoien, J. K. Solberg, and T. Skaland, "Mechanical properties of FeSi (epsilon), FeSi2 (zeta(alpha)) and Mg2Si," *Intermetallics,* vol. 10, pp. 743-750, Aug 2002.

[24] W. B. W. L.C.Davis, G.C.Danielson, "Elastic constants and calculated lattice vibration frequencies of Mg2Sn," *Journal of Physics and Chemistry of Solids,* vol. 28, p. 9, 1967.

[25] P. Gao, I. Berkun, R. D. Schmidt, M. F. Luzenski, X. Lu, P. B. Sarac, E. D. Case, and T. P. Hogan, "Transport and Mechanical Properties of High-ZT Mg2.08Si0.4-x Sn0.6Sb (x) Thermoelectric Materials," *Journal of Electronic Materials,* vol. 43, pp. 1790-1803, Jun 2014.

[26] X. D. Luo, H. Liu, W. L. Xu, and Y. X. Zhu, "Progress on Mg2Si thermoelectric materials," *Advanced Research on Material Science, Enviroment Science and Computer Science Iii,* vol. 886, pp. 71-74, 2014.

[27] P. Sankhla, Kamila, Yasseri, Farahi, Mueller, de Boor, "Mechanical Alloying of Optimized Mg2(Si,Sn) Solid Solutions: Understanding Phase Evolution and Tuning Synthesis Parameters for Thermoelectric Applications," *Applied Energy Materials,* vol. 1, p. 11, 2018.

[28] H. Kamila, P. Sahu, A. Sankhla, M. Yasseri, H. N. Pham, T. Dasgupta, E. Mueller, and J. de Boor, "Analyzing transport properties of p-type Mg2Si-Mg2Sn solid solutions: optimization of thermoelectric performance and insight into the electronic band structure," *Journal of Materials Chemistry A,* vol. 7, pp. 1045-1054, Jan 21 2019.

[29] W. C. Oliver and G. M. Pharr, "An Improved Technique for Determining Hardness and Elastic-Modulus Using Load and Displacement Sensing Indentation Experiments," *Journal of Materials Research,* vol. 7, pp. 1564-1583, Jun 1992.

[30] S. Kamila, Yasseri, Hoang, Farahi, and d. B. Mueller, "Synthesis of p-type Mg2Si1-xSnx with x = 0-1 and optimization of the synthesis parameters," *Materials Today: Proceedings,* vol. 8, p. 9, 2019.

[31] M. E. Launey and R. O. Ritchie, "On the Fracture Toughness of Advanced Materials," *Advanced Materials,* vol. 21, pp. 2103-2110, May 25 2009.

[32] P. Vivekanandhan, R. Murugasami, and S. Kumaran, "Microstructure and mechanical properties of magnesium silicide prepared via spark plasma assisted combustion synthesis," *Materials Letters,* vol. 231, pp. 109-113, Nov 15 2018.

[33] B. H. Kim, J. J. Jeon, K. C. Park, B. G. Park, Y. H. Park, and I. M. Park, "Microstructural characterisation and mechanical properties of Mg-xSn-5Al-1Zn alloys," *International Journal of Cast Metals Research,* vol. 21, pp. 186-192, Aug 2008.

[34] A. Schmitz, J. de Boor, K. Mull, and E. Muller, "Tailoring the mechanical properties of thermoelectric lead telluride by alloying with non-doping calcium," *Journal of Materials Science,* vol. 51, pp. 6933-6943, Jul 2016.

[35] R. He, S. Gahlawat, C. F. Guo, S. Chen, T. Dahal, H. Zhang, W. S. Liu, Q. Zhang, E. Chere, K. White, and Z. F. Ren, "Studies on mechanical properties of thermoelectric materials by nanoindentation," *Physica Status Solidi a-Applications and Materials Science,* vol. 212, pp. 2191-2195, Oct 2015.

[36] L. Zhang, G. Rogl, A. Grytsiv, S. Puchegger, J. Koppensteiner, F. Spieckermann, H. Kabelka, M. Reinecker, P. Rogl, W. Schranz, M. Zehetbauer, and M. A. Carpenter, "Mechanical properties of filled antimonide skutterudites," *Materials Science and Engineering B-Advanced Functional Solid-State Materials,* vol. 170, pp. 26-31, Jun 15 2010.

[37] G. Rogl, A. Grytsiv, M. Gurth, A. Tavassoli, C. Ebner, A. Wunschek, S. Puchegger, V. Soprunyuk, W. Schranz, E. Bauer, H. Muller, M. Zehetbauer, and P. Rogl, "Mechanical properties of half-Heusler alloys," *Acta Materialia,* vol. 107, pp. 178-195, Apr 1 2016.

[38] L. D. Zhao, B. P. Zhang, J. F. Li, M. Zhou, W. S. Liu, and J. Liu, "Thermoelectric and mechanical properties of nano-SiC-dispersed Bi2Te3 fabricated by mechanical alloying and spark plasma sintering," *Journal of Alloys and Compounds,* vol. 455, pp. 259-264, May 8 2008.

[39] J. Eilertsen, M. A. Subramanian, and J. J. Kruzic, "Fracture toughness of Co4Sb12 and In0.1Co4Sb12 thermoelectric skutterudites evaluated by three methods," *Journal of Alloys and Compounds,* vol. 552, pp. 492-498, Mar 5 2013.